

# *Symbolic template iterations of complex quadratic maps*

**Anca R#dulescu & Ariel Pignatelli**

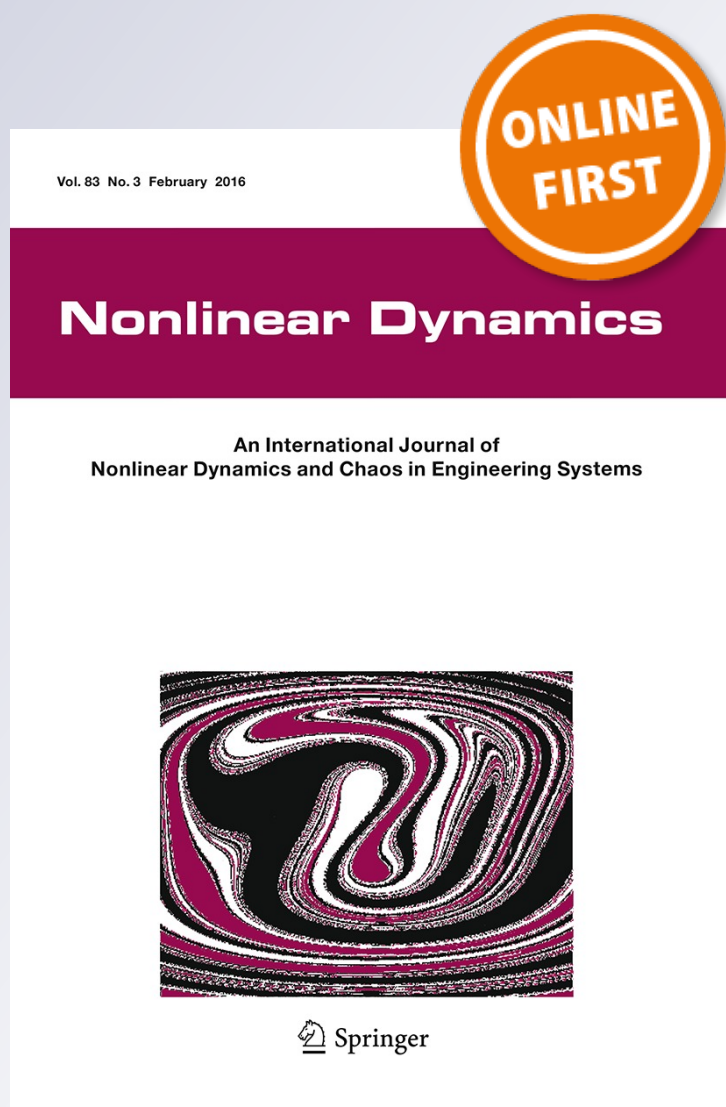
## **Nonlinear Dynamics**

An International Journal of Nonlinear  
Dynamics and Chaos in Engineering  
Systems

ISSN 0924-090X

Nonlinear Dyn

DOI 10.1007/s11071-016-2626-3



**Your article is protected by copyright and all rights are held exclusively by Springer Science +Business Media Dordrecht. This e-offprint is for personal use only and shall not be self-archived in electronic repositories. If you wish to self-archive your article, please use the accepted manuscript version for posting on your own website. You may further deposit the accepted manuscript version in any repository, provided it is only made publicly available 12 months after official publication or later and provided acknowledgement is given to the original source of publication and a link is inserted to the published article on Springer's website. The link must be accompanied by the following text: "The final publication is available at [link.springer.com](http://link.springer.com)".**

# Symbolic template iterations of complex quadratic maps

Anca Rădulescu · Ariel Pignatelli

Received: 19 May 2015 / Accepted: 15 January 2016  
 © Springer Science+Business Media Dordrecht 2016

**Abstract** The behavior of orbits for iterated polynomials has been widely studied since the dawn of discrete dynamics as a research field, in particular in the context of the complex quadratic family  $f: \mathbb{C} \rightarrow \mathbb{C}$ , parametrized as  $f_c(z) = z^2 + c$ , with  $c \in \mathbb{C}$ . While more recent research has been studying the orbit behavior when the map changes along with the iterations, many aspects of non-autonomous discrete dynamics remain largely unexplored. Our work is focused on studying the behavior of pairs of quadratic maps (1) when iterated according to a rule prescribed by a binary template and (2) when the maps are organized as nodes in a network, and interact in a time-dependent fashion. We investigate how the traditional theory changes in these cases, illustrating in particular how the hard-wired structure (the symbolic template, and respectively the adjacency graph) can affect dynamics (behavior of orbits, topology of Julia and Mandelbrot sets). Our current manuscript addresses the first topic, while the second topic is the subject of a subsequent paper. This is of potential interest to a variety of applications (including genetic and neural coding), since (1) it investigates how an occasional or a reoccurring error

in a replication or learning algorithm may affect the outcome and (2) it relates to algorithms of synaptic restructuring and neural dynamics in brain networks.

**Keywords** Julia set · Non-autonomous iterations · Symbolic template · Connectedness · Hausdorff measure · Hybrid Mandelbrot set · Propagating error · Parameter sensitivity · DNA replication

## 1 Introduction

### 1.1 Discrete dynamics of the quadratic family

The family of logistic maps has been over the years one of the most studied examples in the theory of discrete dynamical systems. In the context of real interval maps, typically parametrized as  $f_\mu: [0, 1] \rightarrow [0, 1]$ ,  $f_\mu(x) = \mu x(1 - x)$ , for  $\mu \in [0, 4]$ , results from kneading theory classify the possible orbits, and provide a relationship between the combinatorics of critical orbits and the complexity of the corresponding map (measured, for example, via its topological entropy). In the context of complex functions  $f_c: \mathbb{C} \rightarrow \mathbb{C}$ ,  $f_c(z) = z^2 + c$ , for  $c \in \mathbb{C}$ , results going all the way back to the original theory of Fatou and Julia describe thoroughly the behavior of the orbits in the dynamic complex plane, as well as phenomena in the parameter plane. On the practical side, discrete iterations in general, and the dynamics of quadratic functions in particular, have been used to model natural processes. For

A. Rădulescu (✉)  
 Department of Mathematics, State University of New York  
 at New Paltz, New Paltz, NY 12561, USA  
 e-mail: radulesa@newpaltz.edu

A. Pignatelli  
 Department of Mechanical Engineering, SUNY New Paltz,  
 New Paltz, NY 12561, USA

example, the quadratic family has been used for more than a decade to model integrate and fire neurons [2,9], and iterations of simple discrete maps are the ideal candidate for modeling replication in genetic algorithms.

The prisoner set of a map  $f$  is defined as the set of all points in the complex dynamic plane, whose orbits are bounded. The escape set of a complex map is the set of all points whose orbits are unbounded. The Julia set of  $f$  is defined as their common boundary  $J(f)$ . The filled Julia set is the union of prisoner points with their boundary  $J(f)$ .

For polynomial maps, it has been shown that the connectivity of a map's Julia set is tightly related to the structure of its critical orbits (i.e., the orbits of the map's critical points). Due to extensive work spanning almost one century, from Julia [13] and Fatou [10] until recent developments [1, 15], we now have the following:

**Fatou–Julia Theorem** *For a polynomial with at least one critical orbit unbounded, the Julia set is totally disconnected if and only if all the bounded critical orbits are aperiodic.*

### 1.2 Random iterations of quadratic maps

In nature, it is unlikely that systems evolve according to the same identical dynamics along time. Rather, one expects that occasional or periodic errors may be made in the iteration process, or even that the iteration scheme may change in time, according to the system's new needs as it is adapting. Therefore, a more realistic mathematical context to model such phenomena is to consider time-dependent (non-autonomous) iterations, in which the iterated map may change between steps, evolve in time, or appear (with variable frequency) in conjunction with other maps in the iteration.

Random iterations have been studied since the early 1990s, starting with the pioneering work of Fornæss and Sibony [11]. More recent work has been further addressing dynamic of the system and topological properties of the Julia and Mandelbrot set in the context of non-autonomous iterations [4,5,23]. Some studies have looked in particular at how the traditional theory extends when alternating two quadratic complex maps [6,7] and showed that alternation is sufficient to break the dichotomy in the classical single-map case. For one iterated map of degree two [3,8], the Fatou–Julia Theorem implies that the Julia set is

either totally connected, for values of  $c$  in the Mandelbrot set (i.e., if the orbit of the critical point 0 is bounded), or totally disconnected, for values of  $c$  outside of the Mandelbrot set (i.e., if the orbit of the critical point 0 is unbounded). For alternated maps, Danca et al. showed that the Julia set can be disconnected without being totally disconnected [7]. They further related this extension to the Fatou–Julia theorem for complex polynomials of degree four and showed that alternated Julia sets exhibit graphical alternation.

In our work, we are looking at the iteration process of two different functions,  $f_{c_0}$  and  $f_{c_1}$ , according to a general binary symbolic sequence, in which the zero positions correspond to iterating the function  $f_{c_0}$  and the one positions correspond to iterating the function  $f_{c_1}$ . We view this as a more appropriate framework for replication or learning algorithms that appear in nature, with patterns that evolve in time, and which may involve occasional, random, or periodic “errors”. We investigate, primarily from a visual and numerical perspective, the questions that arise for random complex iterations of two maps. While we relate our results with existing general results in non-autonomous iterations, our interest resides primarily in understanding the dependence of the dynamic behavior on three different aspects of the system's hardwiring: (1) the complex parameter pair  $(c_0, c_1)$  that fixes the iterated maps; (2) the fraction (frequency) of 0s versus 1s in the symbolic template which determines the iteration scheme; and (3) the particular succession (timing) of these 0s and 1s along the template.

### 1.3 Definitions and notations

As with the traditional Julia set, we will be working with the complex quadratic family

$$\{f_c : \mathbb{C} \rightarrow \mathbb{C} \mid f_c(z) = z^2 + c, \text{ with } c \in \mathbb{C}\}$$

However, for each iteration process, we will be using a pair of maps in this family,  $f_{c_0}$  and  $f_{c_1}$ , as follows:

**Definition 1.1** Fix  $c_0, c_1 \in \mathbb{C}$ , and a sequence  $\mathbf{s} = (s_n)_{n \geq 0} \in \{0, 1\}^{\mathbb{N}}$  (which we will call the *symbolic template* of the iteration). For any  $\xi_0 \in \mathbb{C}$ , the *template orbit*  $o_{\mathbf{s}}(\xi_0) = (\xi_n)_{n \geq 0}$  is the sequence constructed recursively, for every  $n \geq 0$ , as:

$$\xi_{n+1} = f_{c_{s_n}}(\xi_n)$$

In other words, for each  $n \geq 0$ , we iterate  $f_{c_0}(z) = z^2 + c_0$  if the corresponding entry  $s_n = 0$  in the symbolic template, and we iterate  $f_{c_1}(z) = z^2 + c_1$  otherwise (i.e., if  $s_n = 1$ ). The Julia set for a symbolic template system is naturally defined as an extension of the traditional one:

**Definition 1.2** Fix  $c_0, c_1 \in \mathbb{C}$ . Then we define, for any  $\mathbf{s} \in \{0, 1\}^{\mathbb{N}}$ :

The template prisoner set:

$$P_{c_0, c_1}(\mathbf{s}) = \{\xi_0 \in \mathbb{C} \mid o_{\mathbf{s}}(\xi_0) \text{ is bounded}\}$$

The template escape set:

$$E_{c_0, c_1}(\mathbf{s}) = \{\xi_0 \in \mathbb{C} \mid o_{\mathbf{s}}(\xi_0) \text{ is not bounded}\}$$

The template Julia set:

$$J_{c_0, c_1}(\mathbf{s}) = \partial P_{c_0, c_1}(\mathbf{s}) = \partial E_{c_0, c_1}(\mathbf{s})$$

Since, in order to construct a template Julia set, we need both a complex parameter pair  $(c_0, c_1)$  and a symbolic template, we can consider phenomena in two different parameter spaces: in  $\mathbb{C}^2$  (for a fixed template  $\mathbf{s}$ ) and in the template space of binary sequences  $\{0, 1\}^{\mathbb{N}}$  (for a fixed pair  $(c_0, c_1)$ ). We define two types of ‘‘Mandelbrot’’ sets, as follows:

**Definition 1.3** Fix  $\mathbf{s} \in \{0, 1\}^{\mathbb{N}}$  symbolic sequence. The corresponding (fixed)-template Mandelbrot set is defined as:

$$\mathcal{M}_{\mathbf{s}} = \{(c_0, c_1) \in \mathbb{C}^2 \mid o_{\mathbf{s}}(0) \text{ is bounded}\}$$

**Definition 1.4** Fix  $(c_0, c_1) \in \mathbb{C}^2$ . The corresponding (fixed)-map Mandelbrot set is defined as:

$$\mathcal{M}_{c_0, c_1} = \{\mathbf{s} \in \{0, 1\}^{\mathbb{N}} \mid o_{\mathbf{s}}(0) \text{ is bounded}\}$$

Properties of the fixed template Mandelbrot set have been previously studied for period two templates (i.e., alternating maps). In [6], the authors illustrate the Mandelbrot set as a subset of the quaternion field, as well as some of its two-dimensional cross sections. In our context, we investigate a few directions:

- Assessing the topological (e.g., connectedness) and fractal properties (e.g., Hausdorff dimension of the boundary) of template Mandelbrot sets  $\mathcal{M}_{\mathbf{s}}$ , and how these vary with changing the template.
- Understanding topological and measure theoretical properties of map Mandelbrot sets  $\mathcal{M}_{c_0, c_1}$ , and how these depend on changing the parameters  $c_0$  and  $c_1$ .

Recent studies [4, 17, 23] have made great progress in extending classical dynamical systems properties

to systems obtained by non-autonomous iterations of polynomials. It was shown [24] that the dynamics for randomly iterated complex polynomials are stable over large parameter loci. Systems defined by random iterations have much weaker chaotic features than the dynamics generated by single-map iterations (the chaos of the averaged system disappears, due to the cooperation of the generators [23]). However, they do not lose variety, because of the existence of multiple attractors [24].

Some of these studies have discussed topological properties and have established upper bounds for the Hausdorff dimension of Julia sets defined in this extended context [19]. Of particular interest has been the question of how the topology and geometry of Julia sets are related to the properties of the critical orbits under random iterations. A natural question to ask is whether the classical result for polynomials of degree  $d \geq 2$  (that the Julia set is connected if and only if the polynomial has bounded postcritical set) holds in this more general context. Sumi et al. have been investigating relationships between the planar postcritical set of a non-autonomous iteration of polynomials and the corresponding Julia set [17, 20–22], by addressing the questions in the framework of semigroups of polynomials (and rational maps, more generally) on the Riemann sphere.

One can consider the semigroup  $G = \{g_{i_n} \circ \dots \circ g_{i_1} \mid n \in \mathbb{N}, g_{i_j} \in \Gamma\}$ , generated by the compact subset  $\Gamma$  of polynomials with degree  $\geq 2$ , and then define the Fatou set:

$$F(G) = \{z \in \hat{\mathbb{C}} \mid G \text{ normal in a neighborhood of } z\}$$

and the Julia set associated with this semigroup:

$$J(F) = \hat{\mathbb{C}} \setminus F(G)$$

If one simply requires that the planar postcritical set

$$P(G) = \overline{\bigcup_{g \in G} \{y \in \mathbb{C} \text{ critical value for } g\}}$$

be bounded, the corresponding  $J(G)$  is not necessarily connected (see [20] for a counterexample). However, one may consider the compact space  $\Gamma^{\mathbb{N}} = \{\boldsymbol{\gamma} = (\gamma_1, \gamma_2, \dots) \mid \text{with } \gamma_j \in \Gamma, \forall j \in \mathbb{N}\}$  with the shift map  $\sigma: \Gamma^{\mathbb{N}} \rightarrow \Gamma^{\mathbb{N}}$ , and the cross-product  $\Gamma^{\mathbb{N}} \times \hat{\mathbb{C}}$ , with the canonical projections  $\pi: \Gamma^{\mathbb{N}} \times \hat{\mathbb{C}} \rightarrow \Gamma^{\mathbb{N}}$  and  $\pi_{\hat{\mathbb{C}}}: \Gamma^{\mathbb{N}} \times \hat{\mathbb{C}} \rightarrow \hat{\mathbb{C}}$ . Sumi [21, 22] defined the skew product associated with the family  $\Gamma$  as the map

$$f: \Gamma^{\mathbb{N}} \times \hat{\mathbb{C}} \rightarrow \Gamma^{\mathbb{N}} \times \hat{\mathbb{C}}$$

defined by  $f(\boldsymbol{\gamma}, z) = (\sigma(\boldsymbol{\gamma}), \gamma_1(z))$  (such that  $\pi \circ f = g \circ \pi$ ). It was noted that, for all  $n \in \mathbb{N}$ , the fiberwise restriction  $f_{\boldsymbol{\gamma}}$  on each  $\pi^{-1}(\{\boldsymbol{\gamma}\}) \simeq \hat{\mathbb{C}}$  acts as  $f_{\boldsymbol{\gamma}}^n(z) = \gamma_n \circ \dots \circ \gamma_1(z)$ , so that the dynamics of  $f$  can be established by looking at the dynamics of sequences generated by the family of fiberwise maps  $\{f_{\boldsymbol{\gamma}}\}_{\boldsymbol{\gamma} \in \Gamma^{\mathbb{N}}}$  with the shift map  $\sigma$ . The fiberwise Julia set  $J^{\boldsymbol{\gamma}}(f)$  can thus be defined for each  $\boldsymbol{\gamma} \in \Gamma^{\mathbb{N}}$ , and it was shown [21] that

$$\pi_{\hat{\mathbb{C}}} \left( \overline{\bigcup_{\boldsymbol{\gamma} \in \Gamma^{\mathbb{N}}} \{\boldsymbol{\gamma}\} \times J^{\boldsymbol{\gamma}}(f)} \right) = J(G)$$

This tightly connects the dynamics of  $f$  to the dynamics of  $G$ . One can further consider the fiber postcritical set of  $f$ :

$$P(f) = \overline{\bigcup_{n \in \mathbb{N}} f^{\circ n}(C(f))} \subset \hat{\mathbb{C}}$$

where

$$C(f) = \left\{ (\boldsymbol{\gamma}, y) \in \Gamma^{\mathbb{N}} \times \hat{\mathbb{C}} \mid y \text{ critical point for } \pi_{\hat{\mathbb{C}}}(f(\boldsymbol{\gamma}, z)) \right\}$$

Sumi [22] showed that if  $\pi_{\hat{\mathbb{C}}}(P(f)) \setminus \{\infty\}$  is bounded in  $\mathbb{C}$ , then the fiberwise Julia sets  $J^{\boldsymbol{\gamma}}(f)$  are connected for any  $\boldsymbol{\gamma} \in \Gamma^{\mathbb{N}}$ .

In our particular case of binary template iterations of quadratic polynomials, we have  $\Gamma = \{f_{c_0}, f_{c_1}\}$ . For any  $\boldsymbol{\gamma} \in \Gamma^{\mathbb{N}}$  (i.e., for a fixed parameter pair  $(c_0, c_1) \in \mathbb{C}^2$  and a given binary template  $\mathbf{s} \in \{0, 1\}^{\mathbb{N}}$ ), we can consider the compact metric space  $X \simeq \overline{\bigcup_{n \in \mathbb{N}} \sigma^n(\mathbf{s})} \subset \{0, 1\}^{\mathbb{N}}$ , and the associated skew product with the shift map  $\sigma: X \rightarrow X$ :

$$f: X \times \hat{\mathbb{C}} \rightarrow X \times \hat{\mathbb{C}}, \quad f(\mathbf{t}, z) = (\sigma(\mathbf{t}), f_{c_{t_1}}(z))$$

for any  $\mathbf{t} = (t_n)_{n \in \mathbb{N}} \in \{0, 1\}^{\mathbb{N}}$  and any  $z \in \hat{\mathbb{C}}$ . Then

$$C(f) = \{(\mathbf{t}, z) \in X \times \hat{\mathbb{C}} \mid z \text{ critical point for } f_{c_{t_1}}\} \\ = \{(\mathbf{t}, 0)\}$$

Hence,  $P(f) = \overline{\bigcup_{n \in \mathbb{N}} \{(\sigma^n(\mathbf{t}), (f_{c_{t_n}} \circ \dots \circ f_{c_{t_1}})(0))\}}$ , so that the fiberwise Julia set  $J^{\boldsymbol{\gamma}}(f)$  is connected if  $\{(f_{c_{t_n}} \circ \dots \circ f_{c_{t_1}})(0), n \in \mathbb{N}\}$  is bounded in  $\mathbb{C}$ , i.e., if the infinite template orbit  $o(\mathbf{t})$  is bounded.

In the following sections, we investigate the template orbits of complex quadratic maps in the family  $f_c(z) = z^2 + c$  for a variety of templates, and we discuss particular questions that appear when performing random iterations within this restricted subset of polynomial generators. The paper is organized as follows: In Sect. 2, we

discuss properties of template Julia sets for fixed templates, both periodic and random. We focus in particular on coupling an arbitrary quadratic map  $f_c(z) = z^2 + c$  with the trivial map  $f_0(z) = z^2$  (whose Julia set is the unit circle). We observe how the connectivity patterns of the fixed template Julia and Mandelbrot sets change when the template itself is modified, to incorporate the two iterations in a different mixture. In Sect. 2.3 in particular, we view the insertion of the second map as an “error” in the iteration process of the first map, and we study the effects of such an error propagating along the template on the structure of the corresponding Julia set. In Sect. 3, we examine properties of Mandelbrot sets. We first focus on template Mandelbrot sets in and on properties of their slices in  $\mathbb{C}^2$ . Then, we view the fixed map Mandelbrot set as a subset of  $[0, 1]^2$ , and we define hybrid Mandelbrot sets. Finally, in Sect. 4, we briefly discuss potential applications of this theory to the modeling of natural systems.

## 2 Template Julia sets

### 2.1 Periodic template Julia sets

In this section, we consider  $k$ -periodic templates:  $\mathbf{s} = [s_1, \dots, s_k]$ , with  $s_{k+j} = s_j$ , for all  $j \geq 0$ . In previous work, Danca et al. have considered iterations of alternating quadratic maps [6, 7]. In our context, this corresponds to considering the two possible symbolic templates of period two  $\mathbf{s} = [01]$  and  $\mathbf{s} = [10]$ .

In the references, the authors show that some basic properties and results are still inherited from the traditional single-map case, but also that some new results emerge. For example, for any alternating orbit, the sequence of even and odd iterates is simultaneously bounded or unbounded, so that the Julia set of the alternated maps  $f_{c_0}$  and  $f_{c_1}$  is the same as the Julia set of the quartic map  $f_{c_1} \circ f_{c_0}$ , for any  $c_0, c_1 \in \mathbb{C}$ . The authors further investigate numerically, graphically, and analytically the relationship between the connectivity type of Julia sets and the boundedness of the critical orbits of alternating maps, verifying the first part of the Fatou–Julia theorem in this case. Other questions, such as conditions for local connectivity of the 4-dimensional Mandelbrot set or of 2-dimensional Mandelbrot slices, remain open to further investigation.

Similar properties extend to periodic template iterations for periods  $k > 2$ , with each template Julia set

identical to a classic Julia set for a degree  $2^k$  polynomial. Notice that a  $j$ -shift  $\sigma$  on a periodic template  $\sigma(\mathbf{s}) = \sigma[s_1, \dots, s_k] \rightarrow [s_{1+j}, \dots, s_{k+j}] = \mathbf{s}^j$  translates as a polynomial transformation of degree  $j$  on the Julia set:

$$J(\mathbf{s}^j) = f_{c_{s_{j-1}}} \circ \dots \circ f_{c_{s_1}}(J(\mathbf{s}))$$

One may look at classes defined by shifts on periodic templates, so that Julia sets within the same class are all related by such transformations. The connectedness properties of a Julia set may be preserved or not by the transformation, depending on the parameters  $c_0$  and  $c_1$ , and on the critical orbit properties produced by their combination.

For templates of period 3 for example, there are 3 such classes (or types):

- (0.) All zero entries:  $\mathbf{s} = [000]$
- (1.) A single one entry:  $\mathbf{s} = [001], \mathbf{s} = [010], \mathbf{s} = [100]$
- (2.) Two one entries:  $\mathbf{s} = [011], \mathbf{s} = [101], \mathbf{s} = [110]$
- (3.) All one entries:  $\mathbf{s} = [111]$

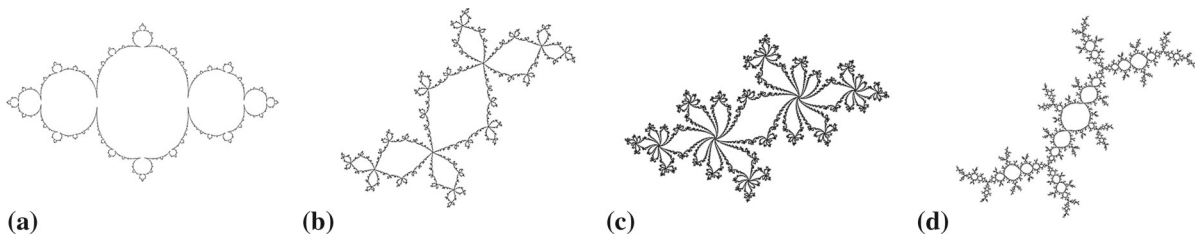
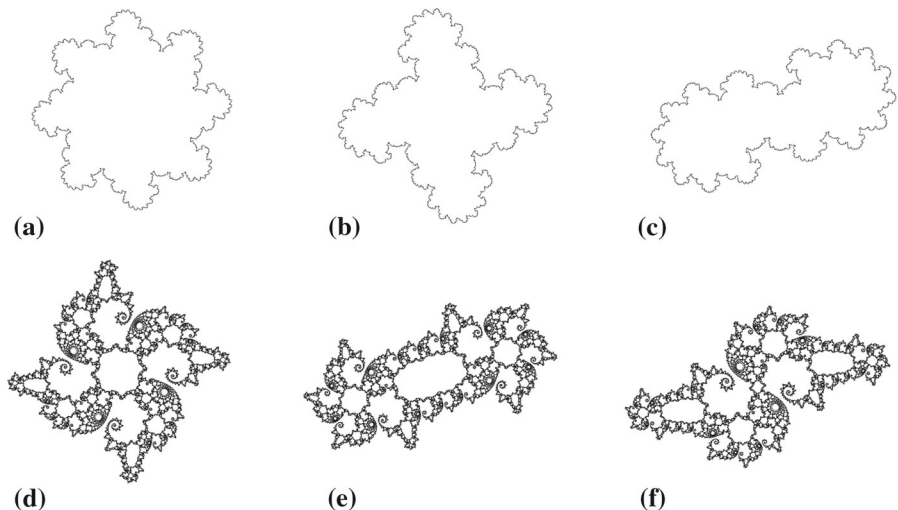


**Fig. 1** Classical Julia sets for four different values of the parameter  $c$ , for which the sets are connected: **a**  $c = -0.75$ ; **b**  $c = -0.117 - 0.76i$ ; **c**  $c = -0.62 - 0.432i$ ; **d**  $c = -0.117 - 0.856i$ .

**Fig. 2** Period 3 template Julia sets for  $c_0 = 0$  and  $c_1 = -0.62 - 0.432i$ , for templates of type 1 (top row) and type 2 (bottom row). **a**  $\mathbf{s} = [011]$ ; **b**  $\mathbf{s} = [101]$ ; **c**  $\mathbf{s} = [110]$ ; **d**  $\mathbf{s} = [001]$ ; **e**  $\mathbf{s} = [010]$ ; **f**  $\mathbf{s} = [100]$



While higher period template Julia sets show similar symmetry properties as observed in the alternating case [6], new questions add to the discussion for higher periods. These refer to understanding how the structure of the periodic template block affects the resulting Julia set, *in combination* with the parameter pair  $(c_0, c_1)$ . The structure of the Julia set is now influenced by three factors: (i) the maps  $c_0$  and  $c_1$ , (ii) the balance of how often one map is iterated versus the other (i.e., the number of 1s versus 0s in the template block), and (iii) the location of these 1s and 0s along the block.

Figures 2, 3, 4, and 5 show, for example, template Julia sets for 3-periodic templates, for combinations of the map  $c_0 = 0$  with the maps  $c_1 = -0.117 - 0.76i$ ,  $c_1 = -0.62 - 0.432i$ ,  $c_1 = -0.5622 - 0.62i$ , and, respectively,  $c_1 = -1 - 0.55i$ . For the first two of these  $(c_0, c_1)$  pairs, the classical Julia sets are shown in Fig. 1; the other two Julia sets are totally disconnected.

The template type seems to affect connectivity of the template Julia set as significantly as the parameters  $(c_0, c_1)$ . It is not surprising that, for fixed  $c_0$  and  $c_1$ ,

We will be using these values in our subsequent illustrations, for combinations of two such functions iterated along a symbolic template

**Fig. 3** Period 3 template Julia sets for  $c_0 = 0$  and  $c_1 = -0.117 - 0.76i$ , for templates of type 1 (top row) and type 2 (bottom row). **a**  $s = [011]$ ; **b**  $s = [101]$ ; **c**  $s = [110]$ ; **d**  $s = [001]$ ; **e**  $s = [010]$ ; **f**  $s = [100]$

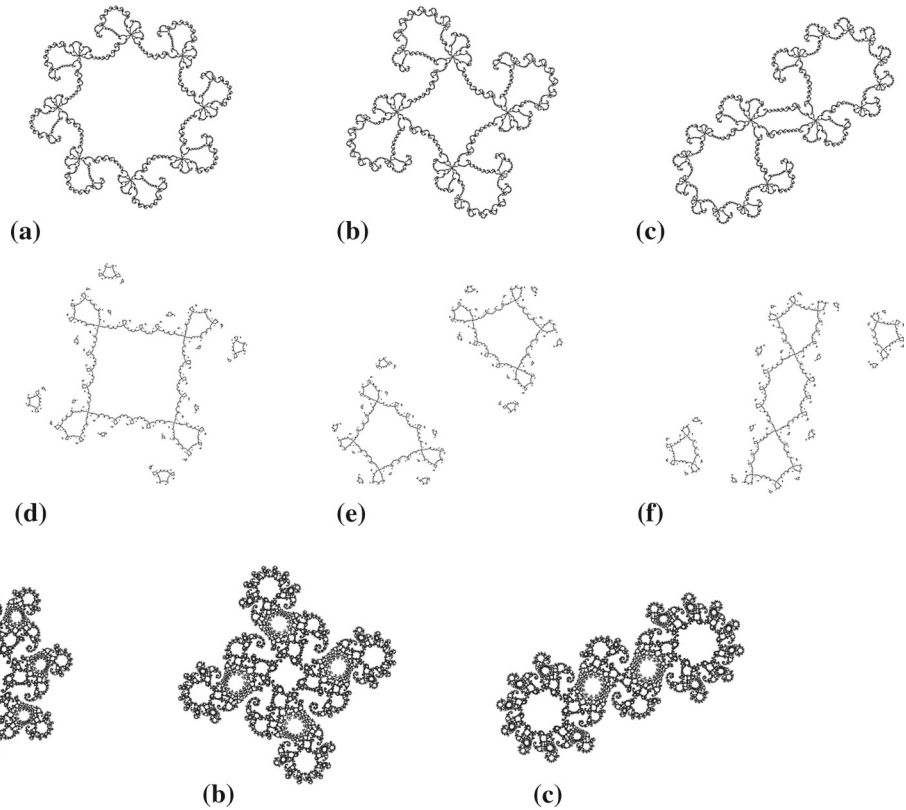


**Fig. 4** Period 3 template Julia sets for  $c_0 = 0$  and  $c_1 = -0.5622 - 0.62i$ , for templates of type 1: **a**  $s = [001]$ ; **b**  $s = [010]$ ; **c**  $s = [100]$ . The Julia sets for the same param-

eter values and templates of type 2, i.e.,  $s = [011]$ ,  $s = [101]$ ,  $s = [110]$ , are totally disconnected (dust)

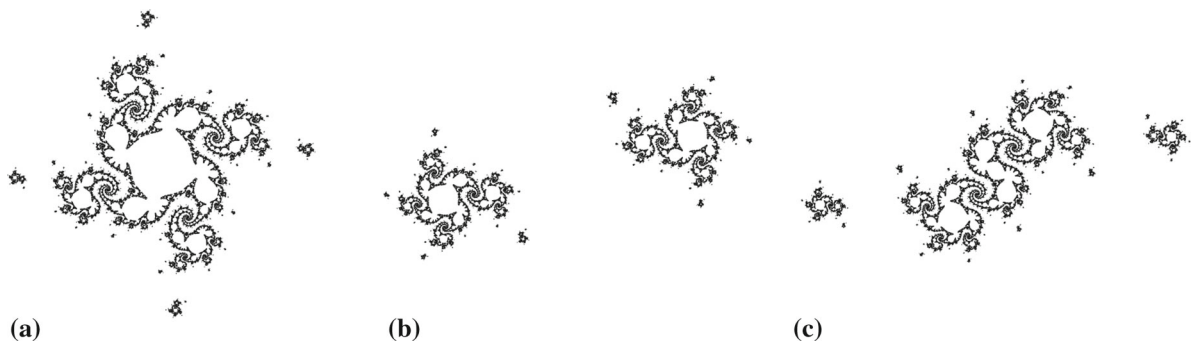


**Fig. 5** Period 3 template Julia sets for  $c_0 = 0$  and  $c_1 = -1 - 0.55i$ , for templates of type 2: **a**  $s = [011]$ ; **b**  $s = [101]$ ; **c**  $s = [110]$ . The Julia sets for the same parameter values and

templates of type 1, i.e.,  $s = [001]$ ,  $s = [010]$ ,  $s = [100]$ , are totally disconnected (dust)

using a different template type (e.g., 1 vs. 2 ones in the 3-periodic case) will affect the connectivity of the Julia set. However, the results may be rather counterintuitive (see Fig. 5). In addition to the template type, changing the position of the 1s along the template may or may

not affect connectivity, as shown in Figs. 2 and 3 for the three different template blocks of type 2. In particular, the folding produced by applying a shift to the template may break or merge connectivity loci, depending on the template and on the complex parameters  $c_0$  and  $c_1$  used.

For  $c_1 = -0.62 - 0.432i$  (Fig. 2),  $c_1 = -0.117 - 0.76i$  (Fig. 3) and  $c_1 = -0.5622 - 0.62i$  (Fig. 4) in combination with  $c_0 = 0$ , the Julia set becomes more disconnected as a result of increasing the contribution of  $c_1$  versus  $c_0$ . Indeed, in the first case, the template Julia set, connected for all cases of type one template (a single one and two zeros), remains connected (although a lot more complex) for all corresponding type 2 templates (two ones and one zero). In the second case, while all type 1 templates render connected Julia sets, these become disconnected for all cases of type 2 template. In the third case, the Julia set for type 1 templates, already disconnected, turns to dust for all type 2 templates. This is somewhat expectable, given the shape of the Julia set for each of these maps considered in isolation (the unit circle for  $c = 0$ , the Julia set shown in Fig. 1c for  $c = -0.62 - 0.432i$ , in Fig. 1b, for  $c = -0.117 - 0.76i$ , and respectively a totally disconnected Julia set for  $c = -0.5622 - 0.62i$ ). However, for  $c_1 = -1 - 0.55i$  (Fig. 5), the opposite happens: The template Julia sets are disconnected, but not totally disconnected for type 2 templates, and become dust for type 1 templates, where the more substantial contribution of the map  $f_{c_0}(z) = z^2$  would suggest otherwise.

### 2.2 Non-periodic template dynamics

The case of periodic templates represents only a first extension, with basic properties expected to replicate quite naturally the theory for iterations of alternated maps. We next consider the more general case, of binary templates which are not necessarily periodic.

In Fig. 6, one non-periodic template was used to create the Julia set for three different combinations of parameters. Perhaps the first thing one notices is that the Julia sets for random templates still exhibit complex

(fractal) structure, symmetry and alternations. However, we need to recall that, in all numerically generated figures, one can only use truncated representations of infinite templates, retaining only a specific number of iterations when representing the Julia set (for example, in all our figures we used 200 iterations). A natural question concerns the variability with the number of iterations (i.e., length of the truncated template) of the resulting approximation for the Julia set.

In Fig. 7, three different non-periodic (randomly generated) templates were used to create the corresponding Julia sets, for three different combinations of parameter values  $(c_0, c_1)$ . Notice that different templates introduce differences in the Julia set as significant as changes in the parameters  $(c_0, c_1)$ . We then fixed template 1 from Fig. 7 and  $c_0 = 0, c_1 = -1$  (that is, we started with the Julia set in the middle left panel). Using the same  $(c_0, c_1)$  pair, we computed the Julia sets for a collection of templates of length 200 with identical entries up to the 10th position. The variations among the Julia sets we obtained this way are clearly much smaller, as illustrated in Fig. 8. To better understand this dependence, we consider the following:

**Definition 2.1** For any  $n \in \mathbb{N}$ , we call the  $k$ -root of a template  $\mathbf{s} = (s_k)$  the finite sequence  $\bar{\mathbf{s}}^k = s_1, \dots, s_k$ . We say that two templates have the same  $k$ -root if they agree up to their  $k$ th position.

Based on our numerical simulations (see Fig. 8), a natural direction of inquiry may be to ask (1) whether increasingly long common roots lead to arbitrarily similar Julia sets, or (2) whether the Julia sets for increasingly long truncated templates approach the Julia set for the infinite template.

**Question 1** Fix a parameter pair  $(c_0, c_1)$ , and a template  $\mathbf{s}$ . Is it true that, for any  $\delta > 0$ , there exists  $n \in \mathbb{N}$

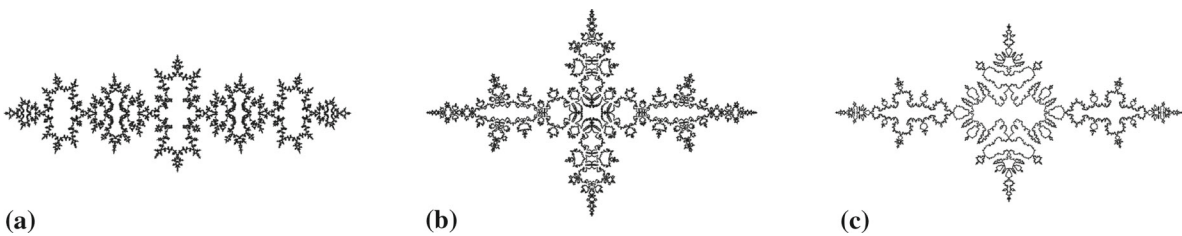


**Fig. 6** Template Julia sets for one fixed non-periodic template (identified as  $\mathbf{s}_1$  in “Appendix 3”), and different pairs  $(c_0, c_1)$ : **a**  $c_1 = -0.75$  and  $c_0 = -1.2$ ; **b**  $c_1 = -1.2$  and  $c_0 = -0.75$ ;

**c**  $c_1 = -1.2$  and  $c_0 = -1$ . For the simulation, the template creating the Julia set was truncated to 200 iterations

**Fig. 7** Template Julia sets for three different randomly generated templates, truncated to 200 iterations (from left to right, we illustrate, respectively, templates  $s_2$ ,  $s_3$  and  $s_4$  from “Appendix 3”). The parameters used are  $c_0 = 0$  and, from top to bottom:  $c_1 = -0.75$  (top),  $c_1 = -1$  (middle) and  $c_1 = 0.375 + 0.333i$  (bottom)

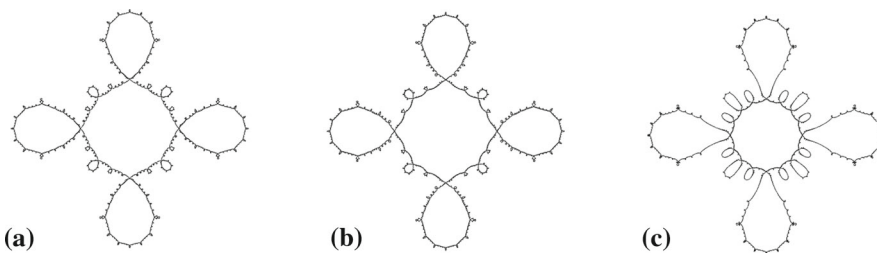
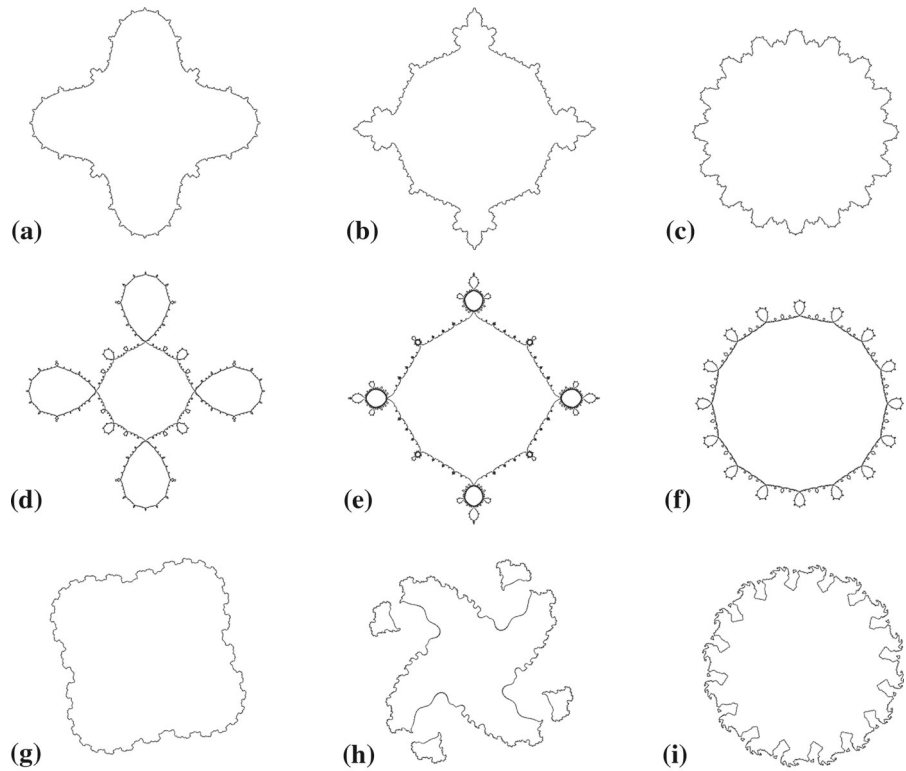


**Fig. 8** Template Julia sets for  $c_1 = -1$  and  $c_0 = 0$ , for three random truncated templates of length 200 with the same root of length  $l = 10$ . From left to right, we show, respectively, templates  $s_2$ ,  $s_5$  and  $s_6$  from “Appendix 3”. The first template (left)

is the same as template 1 in Fig. 7; hence, the corresponding Julia set is identical with that in the middle left panel in the referenced figure

such that, if  $s_1$  and  $s_2$  are two templates with a common  $n$ -root, then

$$d(J_{c_0, c_1}(s_1), J_{c_0, c_1}(s_2)) < \delta$$

where  $d$  represents the Hausdorff distance between two sets?

**Question 2** Fix a parameter pair  $(c_0, c_1)$ . Is it true that, for any  $\delta > 0$ , there exists  $N \in \mathbb{N}$  such that:

$$d(J_{c_0, c_1}(\bar{s}^n) - J_{c_0, c_1}(s)) < \delta, \text{ for } n \geq N$$

These questions relate directly to a well-known result proved by Comerford and Woodard in the context of random iterations of hyperbolic polynomials:

**Theorem [4].** *If a sequence of bounded polynomial sequences which are bounded and hyperbolic with the same constants converges to a bounded polynomial sequence, then the iterated Julia sets also converge in the Hausdorff to the Julia set of the limit sequence.*

Using skew products associated with polynomial semi-groups, Sumi [18] and Sester [16] proved a similar

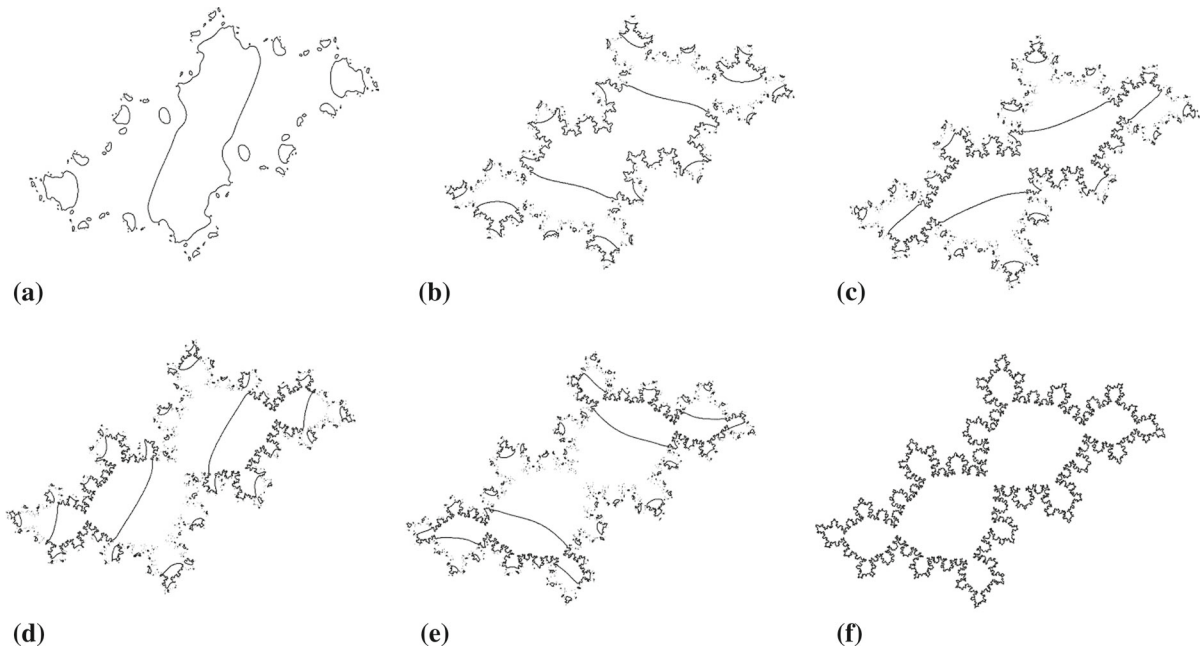


**Fig. 9** Julia set for iterations of the polynomial  $h_1(z) = z^2 + \rho z$  with irrational rotation number  $\rho = e^{2\pi i r}$ , where  $r = \frac{1+\sqrt{5}}{2}$ , in conjunction with the polynomial  $h_2(z) = z^2 + 2z$ . The sets were constructed based on templates of length  $n = 200$ , with the map  $h_1$  being iterated for the zero positions, and the map  $h_2$  for

the one positions. The panels illustrate templates  $s_n = 0^k 1^{n-k}$  for increasing values of  $k$ : **a**  $k = 10$ ; **b**  $k = 50$ ; **c**  $k = 100$ ; **d**  $k = 150$ ; **e**  $k = 195$ ; **f**  $k = 200$ . The Julia sets are not getting closer to the Julia sets for  $s_{200}$  in Hausdorff distance as  $k$  increases

result when assuming semi-hyperbolicity of the skew product. Semi-hyperbolicity is yet a rather strong condition, and one may easily find examples of skew products which are not hyperbolic. The following non-semi-hyperbolic setup represents a class of counterexamples, also constructed by Sumi [21], showing that Hausdorff convergence of the Julia set is no longer guaranteed in the absence of semi-hyperbolicity. Consider the semigroup generated by  $\Gamma = \{h_1, h_2\}$ , where one polynomial  $h_1$  has a Siegel disk, whose center  $\xi_0$  is a repelling fixed point for the second polynomial  $h_2$ . In Fig. 9, we illustrate a few instances of the Julia set along the sequence of templates  $s_n = (0, \dots, 0, 1, 1, \dots)$  (composed of an increasing block of zeros followed by ones), for the quadratic polynomials  $h_1(z) = z^2 + \rho z$ , and  $h_2(z) = z^2 + 2z$ , where  $\rho = e^{2\pi i r}$ , and  $r = \frac{1+\sqrt{5}}{2}$  is the golden ratio. The map  $h_1$  has a fixed point at  $z_0 = 0$  and irrational rotation number; its Julia set has a Siegel disk centered at zero, which is a repelling fixed point for  $h_2$ . As the common root of zeros is getting longer, the Julia sets are not getting closer in the Hausdorff distance, and they are not approaching the Julia set of the map  $h_1$ .

Let us note, however, that this class of counterexamples does not exist within our particular quadratic polynomial family, since an indifferent fixed point  $\xi_0$  for one map  $f_c = z^2 + c$  cannot be a repelling fixed point for another map in the same family. Further work would be required to answer questions 1 and 2, and either establish that the result holds within our particular family without additional hyperbolicity or semi-hyperbolicity conditions, or refute the result by constructing a working counterexample.

### 2.3 Propagating a perturbation

One way to interpret the combination of two maps in the iteration scheme is to think of  $f_{c_1}$  as the desired map, and of  $f_{c_0}$  as an “error,” or “perturbation” in the desired iteration. In this context, an all 1 template corresponds to a “perfect” replication process, in which a specific map  $f_{c_1}$  is iterated identically for a (large or infinite) number of times, and any number of zero entries in the template correspond to as many intrusions

of the erroneous map  $f_{c_0}$  in this iteration process. This intrusion can be periodic, or may occur at a random sequence of steps. Here, we discuss the changes in the Julia set produced by propagating a single error along a perfect template.

In “Appendix 1,” we illustrate the effects on the Julia set of a single propagating error, for a few combinations of maps. In Figs. 14 and 15, the desired map  $f_{c_1}$  is combined with the trivial map  $f_0(z) = z^2$ , while in Fig. 16, the error is a different (and unrelated) function, with complex parameter  $c_0 \neq 0$ . In Fig. 17, the error is a small perturbation of the original function, i.e.,  $c_0 = c_1 + \epsilon$ , with a small  $\epsilon \in \mathbb{C}$ .

In light of the discussion in the previous section, longer common roots seem to lead to more similar Julia sets. The impact of the same error on the Julia set is more substantial when the error occurs earlier in the iteration process. In fact, the Julia sets start to be reminiscent of the correct Julia set less than 50 iterations through the template length. Along the way, however, the connectivity and symmetry of the erroneous Julia changes at each step, sometimes in unexpected and counterintuitive ways. Notice, for example, that the small perturbation to  $c_1$  (in Fig. 17) has at each step an effect on the Julia set which is comparable with that of a much larger perturbation (in Figs. 15, 16). This promotes the possibility that, in such a replication process, the timing of the error is equally or even more important than the size of the error.

### 3 Mandelbrot sets

Since, as in the original reference, we are using two iterated maps in combination, the template Mandelbrot set can be seen as a 2-dimensional complex object (the locus of  $(c_0, c_1) \in \mathbb{C}^2$  for which the template orbit of zero is bounded). One may study topological properties of template Mandelbrot sets, and their dependence on template type (periodic or non-periodic). One way to visualize the Mandelbrot set for a fixed template is by looking at a lattice of 2-dimensional slices, each representing the behavior with respect to  $c_1$  for a fixed  $c_0$  (see in Fig. 18 in “Appendix 2”). We are, however, more interested in understanding how the fractal structure of the set boundary (measured by its Hausdorff dimension) changes when varying the template type, density or regularity.

We first observed the structure of template Mandelbrot sets for periodic templates. When we tracked the fractality of the boundary of template Mandelbrot sets, we found a consistent trend of alternation between boundary regions with high and low complexity (which we illustrate in Fig. 10, using consecutive zooms into various regions along the boundary).

We then looked at the Mandelbrot boundary in the case of non-periodic templates. Due to the lack of regularity in the occurrences of  $c_0$  and  $c_1$  in the template, the fractal dimension of the template Mandelbrot boundary seems to be lower than that for periodic templates, but more uniform along the whole set boundary (Fig. 11), in contrast with the situation for periodic templates, where high Hausdorff dimension regions were interposed with portions of low Hausdorff dimension.

This is not too surprising: The phenomenon of cooperation between generating maps has been already proposed by Sumi [23] as a contributor to decreasing the chaos in the overall system. However, this phenomenon was only described in the context of averaged behavior over all initial conditions. Our numerical result seems to support a similar effect of randomness “smoothing out the chaotic structure” along the boundary of the Mandelbrot set. A better understanding of the latter as well as a possible relationship between these two phenomena may become clearer with a more rigorous investigation of the topology of template Mandelbrot slices.

Next, we want to suggest two alternative ways of viewing the fixed map Mandelbrot set, and of observing how the template affects the properties of the orbit  $o_s(0)$ , for a fixed parameter pair  $(c_0, c_1) \in \mathbb{C}$ . As a book-keeping method for truncated templates, we propose to consider each binary sequence of length  $L$  as equivalent to the binary representation of a real number  $0 \leq n \leq 1$  with precision  $2^{-L}$ . In other words, we can consider, for each  $0 \leq a \leq 1$ , its binary expansion up to its  $L$ th binary digit, always choosing the infinite expansion (when it is the case). For fixed  $c_0$  and  $c_1$ , we can use each expansion as the symbolic template, and check whether the orbit  $o_s(0)$  is bounded or not. We can construct the function:  $F: [0, 1] \rightarrow \{0, 1\}$ , given by  $F(n) = 1$ , if  $o_s$  is bounded, and  $F(n) = 0$ , if  $o_s(0)$  is not bounded. In Fig. 12, we show a few such representations, for various choices of the complex parameter pair  $(c_0, c_1)$ , connecting the discontinuous points in order to make the structure of the set more visible. It is clear that the behavior of the fixed map Mandelbrot set  $F^{-1}(1)$  depends crucially

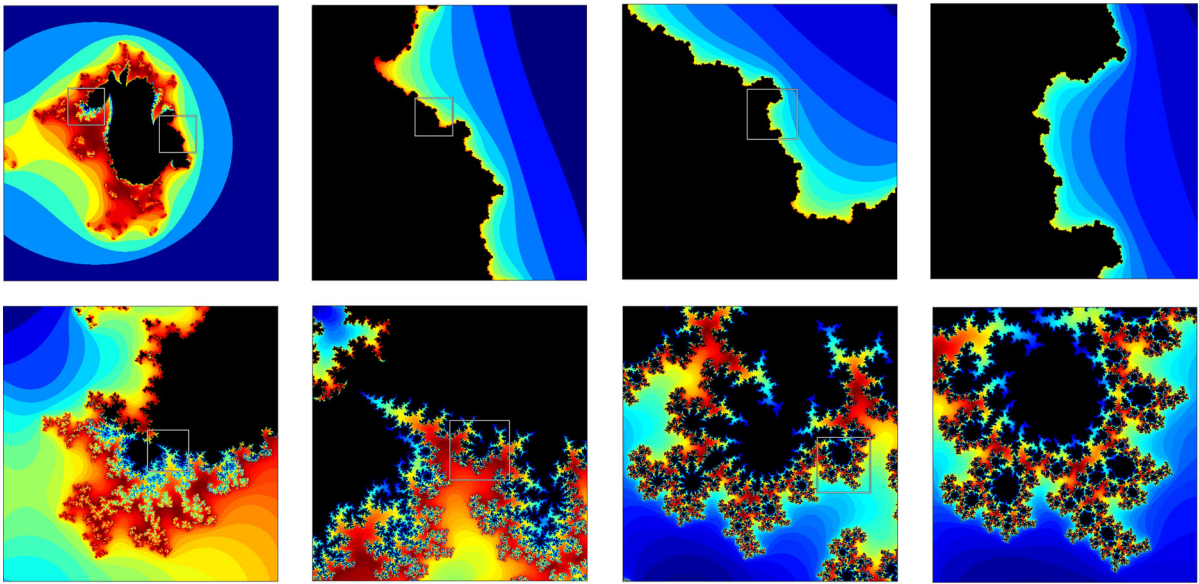


**Fig. 10** Template Mandelbrot slice for  $c_1 \in \mathbb{C}$ , for the periodic template [011] and fixed  $c_0 = -0.2 + 0.6i$ . The figure shows two progressively zoomed-in windows: one with low, the other with high Hausdorff dimension along the boundary. Three consecutive zoom-ins of the first instance are represented on *top*,

and four zoom-ins of the second situation are represented on the *bottom*. The pattern persists at higher and higher levels, suggesting an alternation of high and low dimension intervals along the boundary of the set

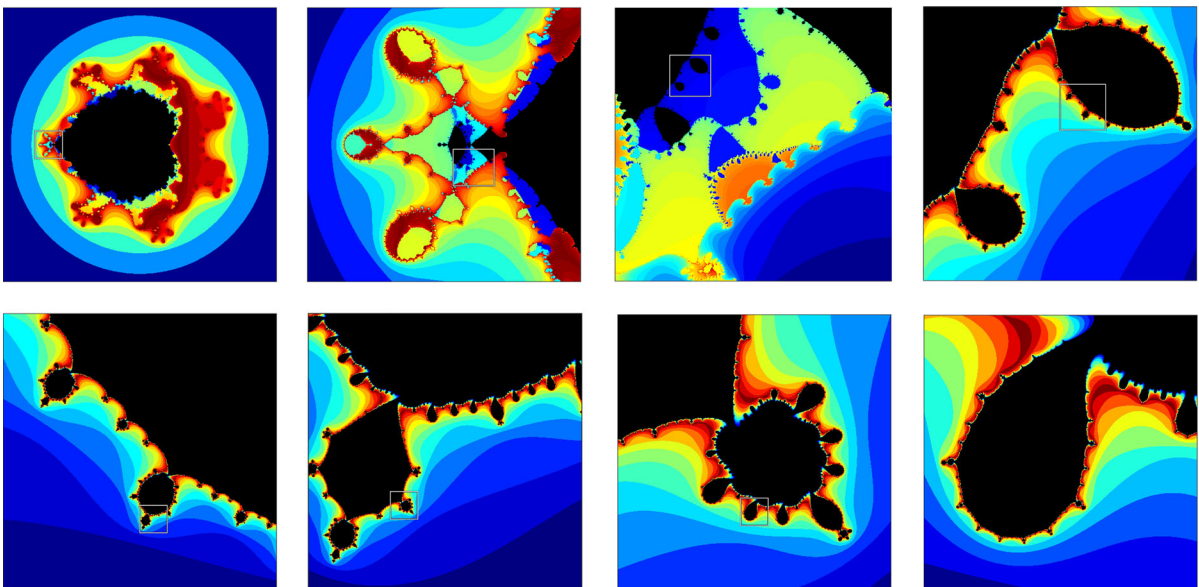


**Fig. 11** Template Mandelbrot slice for  $c_1$ , for a template of length 200 generated at random (template  $s_7$  from “Appendix 3”). The zeros in the template correspond to the map  $c_0 = 0$  and the ones to the respective map  $c_1$ . Each *panel* shows at higher

resolution a zoomed-in window, marked on the preceding panel. The structure persists at higher and higher levels, suggesting the preservation of fractal features in the Mandelbrot set, even for random templates

**Fig. 12** Fixed map Mandelbrot sets, for different parameter pairs  $(c_0, c_1) \in \mathbb{C}$ .  
**a**  $c_1 = -0.117 - 0.76i$ ,  $c_0 = -0.5622 - 0.62i$ ;  
**b**  $c_1 = -0.5622 - 0.62i$ ,  $c_0 = -0.5622 - 0.62i$ ;  
**c**  $c_1 = -0.117 - 0.76i$ ,  $c_0 = -0.75$ ; **d**  $c_1 = -0.75$ ,  $c_0 = -0.117 - 0.856i$ . We created binary expansions of length  $L = 15$  for the numbers in the unit interval  $[0, 1]$  (represented along the  $x$ -axis), which we then used as the symbolic templates for the iteration process

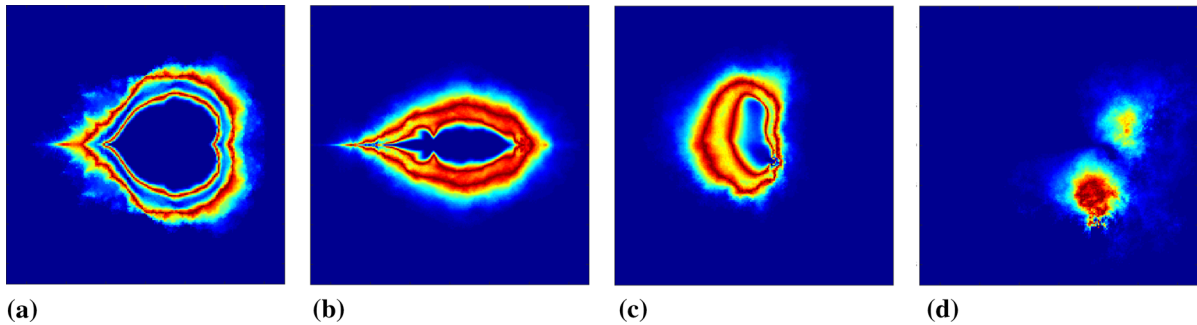
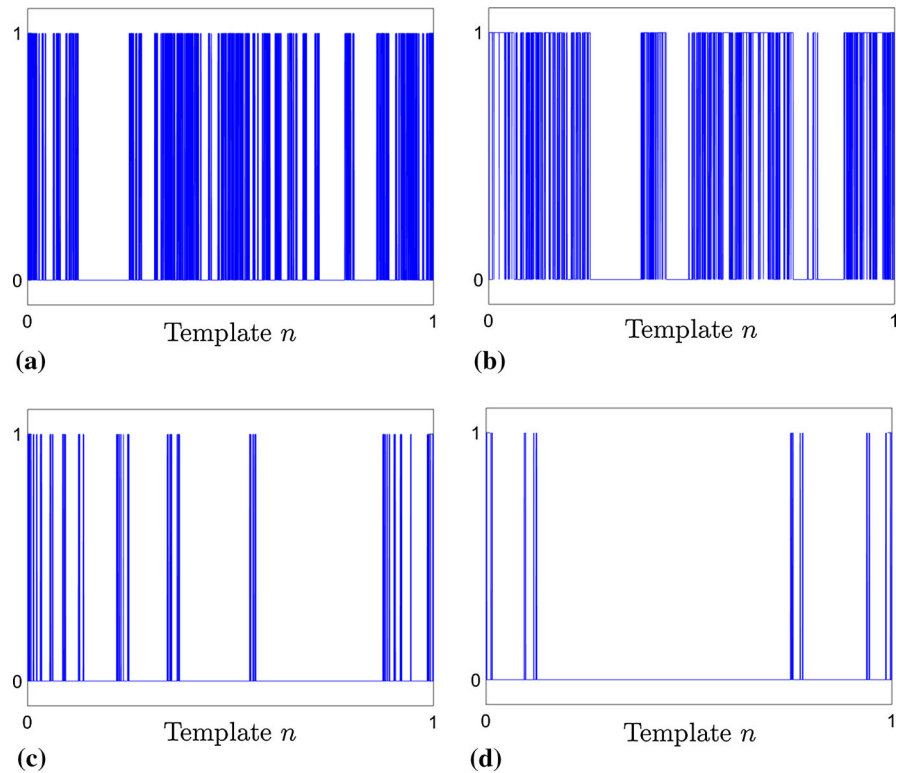


**Fig. 13** Hybrid Mandelbrot sets for different values of  $c_0$ : **a**  $c_0 = 0$ ; **b**  $c_0 = -0.75$ ; **c**  $c_0 = 0.375 + 0.333i$ ; **d**  $c_0 = i$ . For each  $c_1$  (represented in the complex plane), we used colors

to illustrate how many templates of length  $L = 20$  lead to a bounded orbit  $o_s(0)$ . The color spectrum goes from blue (low) to red (high). (Color figure online)

on the parameter values. However, an analysis of its topological properties (accumulation points, density etc.), or its measure in  $[0, 1]$  remains open for further studies of map Mandelbrot sets as fibered sets over  $[0, 1]$ .

Another interesting representation can be obtained as a hybrid of fixing the map and fixing the template. With a fixed  $c_0$ , we can measure, for each different value of  $c_1 \in \mathbb{C}$ , how likely it is (i.e., for how many of all templates of a certain length) that the orbit  $o_s(0)$  is

bounded. In Fig. 13, we show a few such slices in the  $c_1$  complex plane, with the colors representing the number of templates for which  $o_s(0)$  is bounded. Notice the structure reminiscent of the classical Mandelbrot set of the hybrid slice  $c_0 = 0$ , with the boundary fractal behavior smoothed out. This is also potentially related to the phenomena of “averaging out the chaos” described by Sumi, except the averaging is performed here in the parameter plane, rather than over the set of initial conditions.

## 4 Discussion

### 4.1 Comments and future work

In this paper, we described a few ideas which are, to the best of our knowledge, new aspects of existing problems in random discrete dynamics. We defined template iterations of two quadratic maps, and we used standard numerical algorithms to investigate the Julia and Mandelbrot sets of template systems. While this study is a first step in establishing the framework and phrasing some questions, a lot of theoretical work remains to be done, possibly exploring a brand new set of questions in discrete dynamics, requiring new methods from non-autonomous iterations, and the corresponding extensions for the concepts of critical and periodic orbits.

In the meantime, in our computational work we are continuing to investigate generalizations of the Julia set, in particular in the context of networks of interconnected complex quadratic maps. While pairs of coupled logistic maps have been studied before in both real and complex case, we are interested to study the coupled behavior in higher-dimensional networks, with possible applications to understanding dynamics in neural networks. We are focused in particular on understanding the effects of the network architecture (e.g., graph Laplacian) and the dynamic properties of the ensemble as a whole, and on the topology of the “Julia set” of the networked system.

### 4.2 Applications to genetics

Our system can be viewed as a theoretical framework for studying iterated replication mechanisms which are subject to errors at each iteration step, such as DNA replication. When a cell divides, it has to copy and transmit the exact same sequence of billion nucleotides to its daughter cells. While most DNA is typically copied with high fidelity (polymerase enzymes are amazingly precise when performing DNA synthesis), errors are a natural part of DNA replication, with rates of about 1 per  $10^5$  (polymerases sometimes inserting too many or too few, or erroneous nucleotides into a sequence). Human diploid cells have 6 billion base pairs, and each cell division makes about 120,000 errors [14].

Cells have evolved highly sophisticated DNA repair processes, aimed to promptly fix most of these errors.

Some errors are corrected right away, during replication, through a repair process known as proofreading. Proofreading fixes about 99% of the errors, but that is still not sufficient for normal cell functioning. Some errors are corrected after replication, in a process called mismatch repair. Incorrectly paired nucleotides that still remain following mismatch repair become permanent mutations after the next cell division: Once established, the cell no longer recognizes them as errors [14], passing them on to next generations of cells and (if the errors occur in gametes) even to next generations of the organism.

When the genes for the DNA repair enzymes themselves become mutated (the iterated function changes in the long term), mistakes begin accumulating at a much higher rate. Mutation rates vary substantially among taxa, and even among different parts of the genome in a single organism. Scientists have reported mutation rates as low as 1 per  $10^6$ – $10^9$  nucleotides, mostly in bacteria, and as high as 1 per  $10^2$ – $10^3$  nucleotides in humans [12]. Cells accumulate mutations as they divide. Even mutation rates as low as  $10^{-10}$  can accumulate quickly over time, particularly in rapidly reproducing organisms like bacteria.

In genetics, polymerases replicate identically the DNA strand at division, which in turn governs the development of the cell, and is passed on at the next cell division. In our model, the original system/cell (in our case, the complex  $z$ -plane) is programmed to evolve according to a certain sequence of steps, leading to emergence of some features and extinction of others. For example, an initial  $\xi_0$  which iterates to  $\infty$  may represent a cell feature which becomes unsustainable after a number of divisions, while an initial  $\xi_0$  which is attracted to a simple periodic orbit may represent a feature which is too simple to be relevant or efficient for the cell. Then the points on the boundary between these two behaviors (i.e., the Julia set) may be viewed as the optimal features, allowing the cell to perform its complex function. An error at the level of the iteration function at one particular iteration step is equivalent to a mutation that occurred at one of the cell division steps. The new cell/complex plane is then used as template for the next iteration/division; one can study how the features of the cell are affected in the long term, when such an error passes undetected by the repair mechanisms. In our paper, we considered situations where such an occurrence is singular, random/occasional, or periodic. It is clear that mutations accumulated over a long period

of time may lead to serious changes in the structure of the later cells (different topological properties of the Julia set). Our model also addresses the timing when the errors occur and illustrates how a mutation in the early iterative stages can lead to substantially more dramatic consequences on the result (Julia set) than the same error if it happens later in the process.

The construction of mathematical models to help understand DNA replication and repair would be highly desired, since these are crucially important and complex mechanisms to study and understand. In eukaryotic cells, accumulating mutations can lead to cancer. However, if DNA replication were perfect (mutation-free), there would be no genetic variation. Therefore, successful organisms had to construct optimal mechanisms, providing efficient DNA repair, but also enough variability for evolution to continue. A mathematical framework would be ideal for posing and contextualizing such questions.

**Acknowledgments** The authors would like to thank Mark Comerford, Hiroki Sumi and Rich Stankewitz for the useful discussions.

**Appendix 1: Effect of a propagating error along the template**

See Figs. 14, 15, 16, and 17.

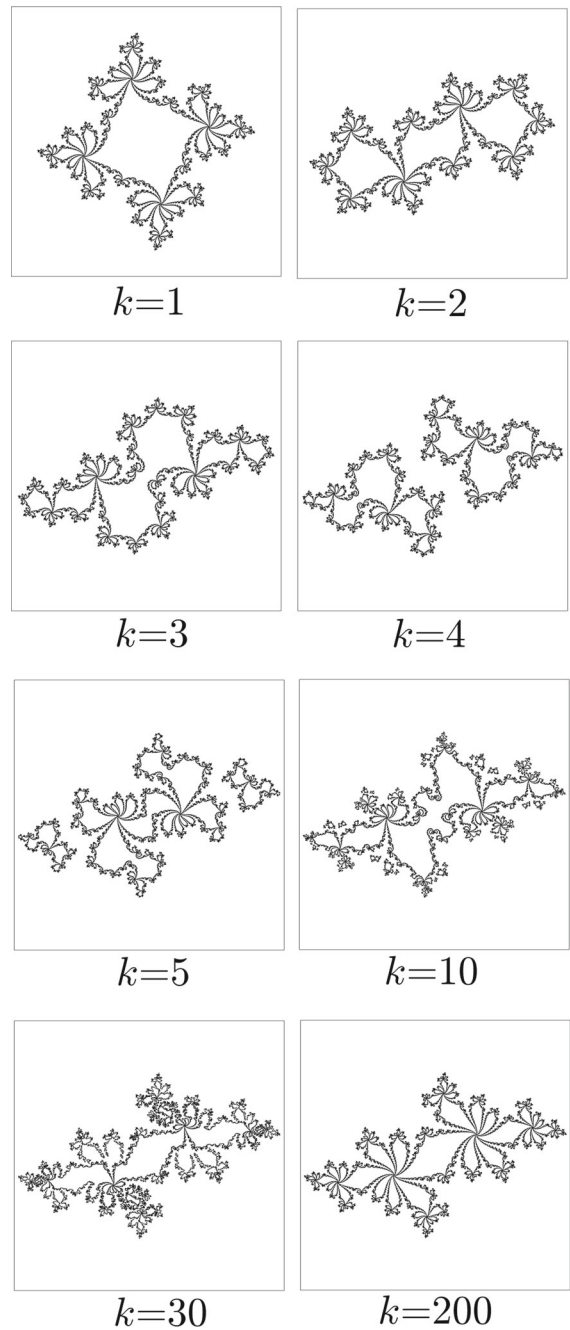


**Fig. 14** Effect of error propagation on the Julia set for the desired function with parameter  $c_1 = -0.62 - 0.432i$  (whose classical Julia set is shown in Fig. 1c) and error parameter  $c_0 = 0$  (whose classical Julia set is the unit circle). The perturbation of  $f_{c_1}$  to  $f_{c_0}$  was introduced successively at the iterations  $k = 1, 2, 3, 4, 5, 10, 30$ , and  $200$  in a truncated template of length  $N = 200$  (each Julia set is represented in one of the figure panels, from smaller to larger values of  $k$ .)

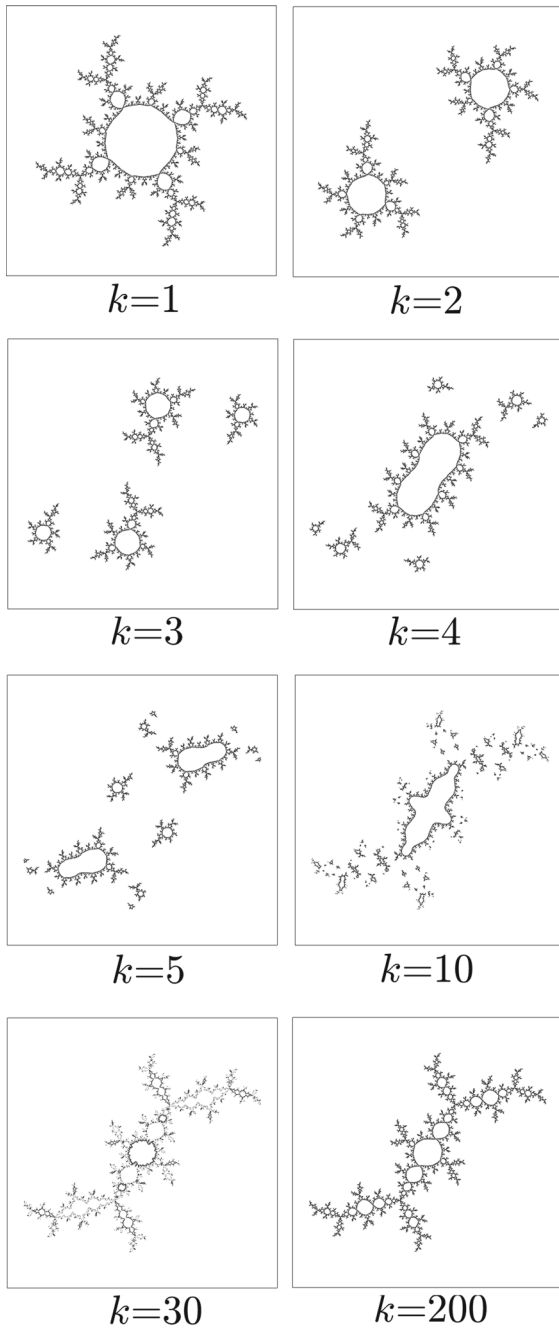


**Fig. 15** Effect of error propagation on the Julia set for the desired function with parameter  $c_1 = -0.117 - 0.856i$  (whose classical Julia set is shown in Fig. 1e) and error parameter  $c_0 = 0$  (whose classical Julia set is the unit circle). The perturbation of  $f_{c_1}$  to  $f_{c_0}$  was introduced successively at the iterations  $k = 1, 2, 3, 4, 5, 10, 30$ , and  $200$  in a truncated template of length  $N = 200$  (each Julia set is represented in one of the figure panels, from smaller to larger values of  $k$ .)

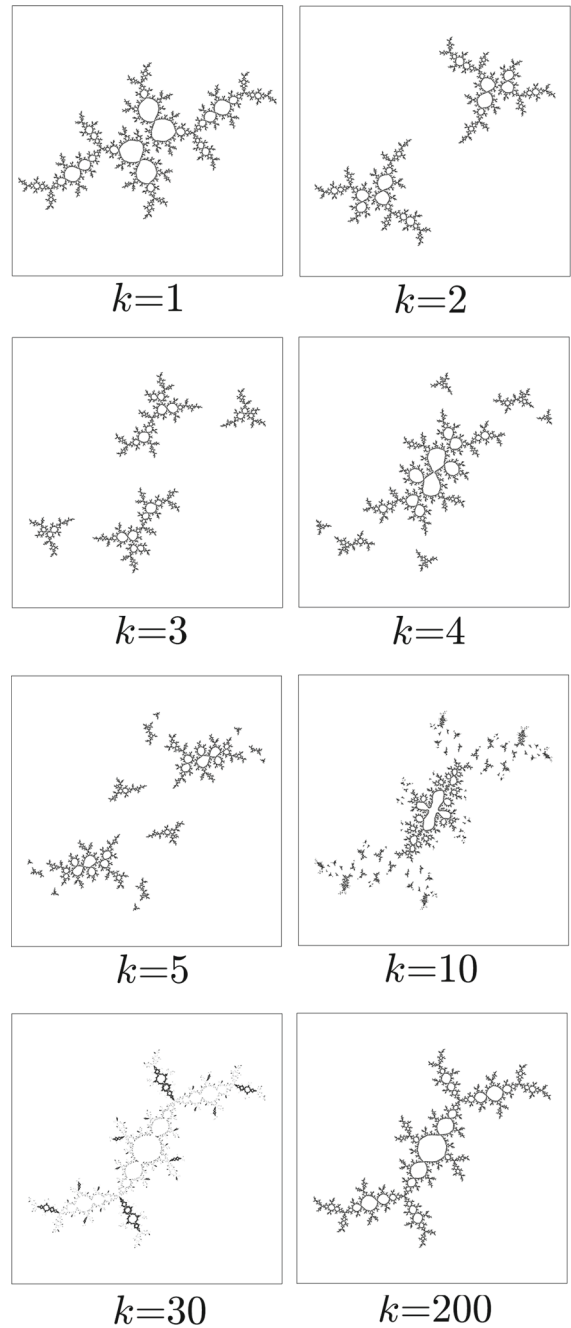
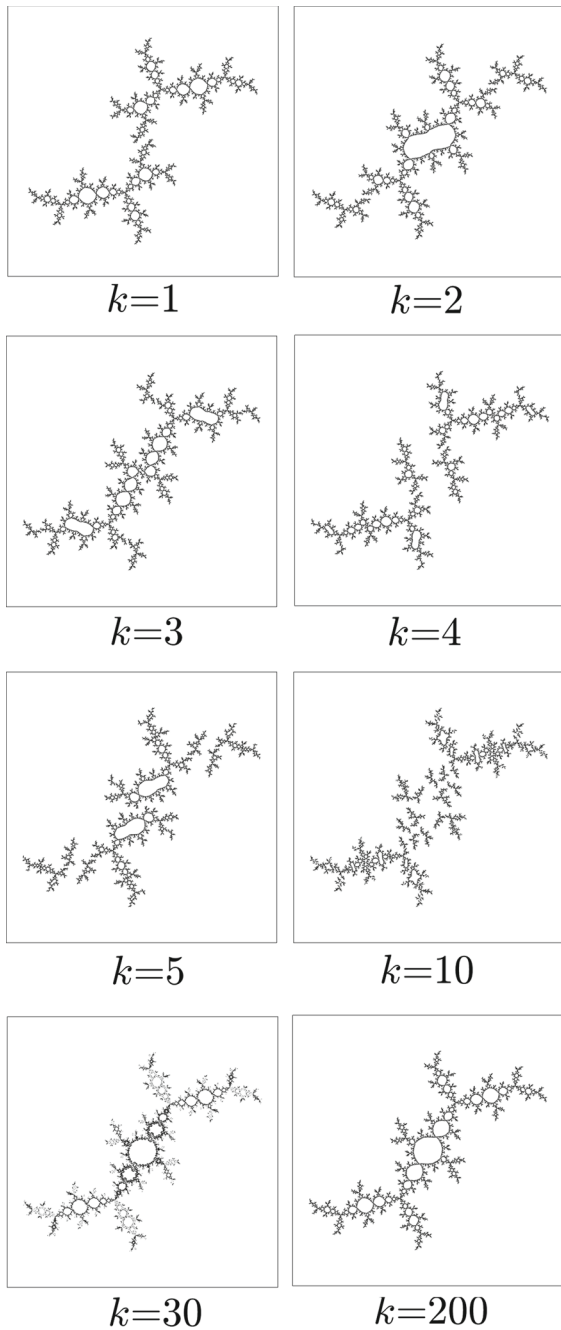


**Fig. 16** Effect of error propagation on the Julia set for the desired function with parameter  $c_1 = -0.117 - 0.856i$  (whose classical Julia set is shown in Fig. 1d) and error parameter  $c_0 = -0.5622 - 0.62i$  (whose classical Julia set is shown in Fig. 1e). The perturbation of  $f_{c_1}$  to  $f_{c_0}$  was introduced successively at the iterations  $k = 1, 2, 3, 4, 5, 10, 30$ , and  $200$  in a truncated template of length  $N = 200$  (each Julia set is represented in one of the figure panels, from smaller to larger values of  $k$ .)

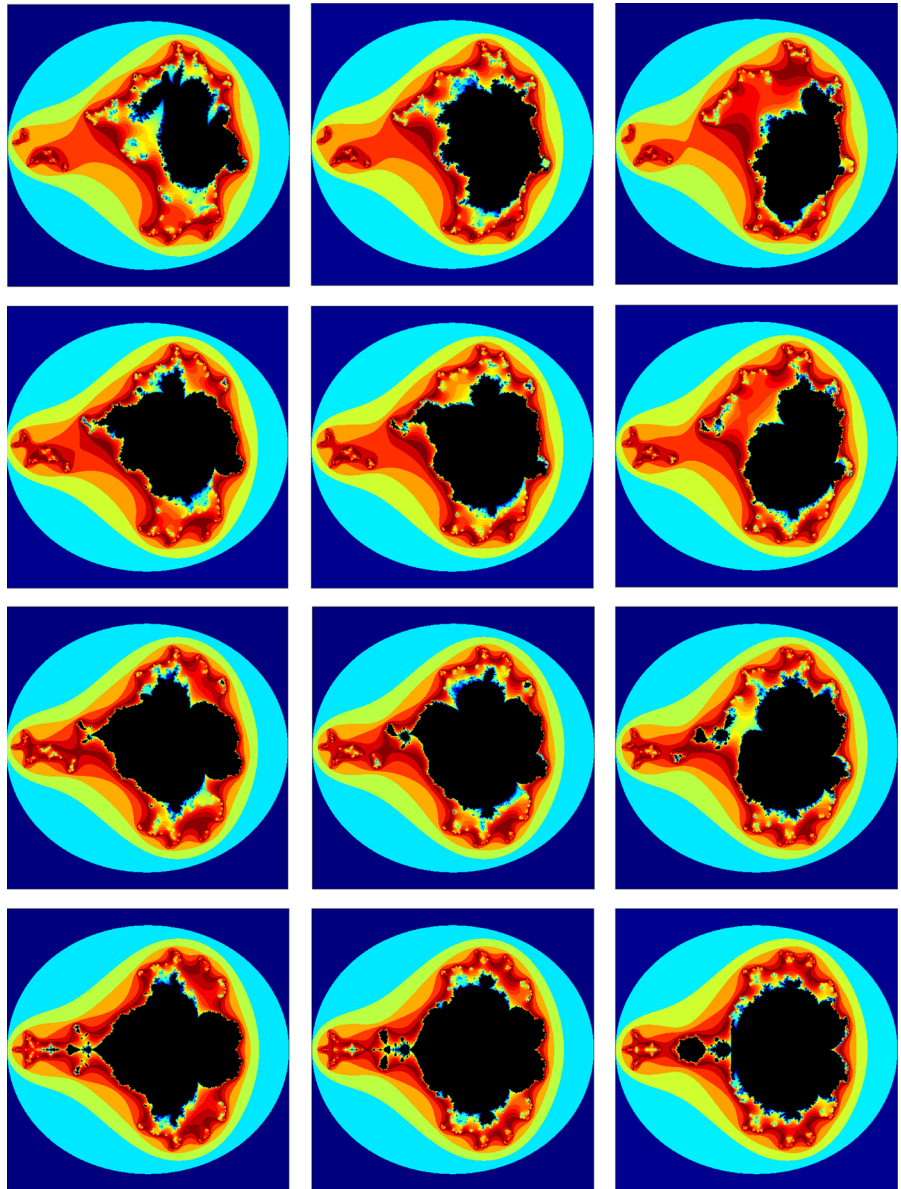


## Appendix 2: Template Mandelbrot slices

See Fig. 18.

**Fig. 17** Effect of error propagation on the Julia set for the desired function with parameter  $c_1 = -0.117 - 0.856i$  (whose classical Julia set is shown in Fig. 1d) and error parameter  $c_0 = c_1 + \varepsilon$ , where  $\varepsilon = 0.1 + 0.1i$  (a small complex perturbation of  $c_1$ ). The perturbation of  $f_{c_1}$  to  $f_{c_0}$  was introduced successively at the iterations  $k = 1, 2, 3, 4, 5, 10, 30$ , and  $200$  in a truncated template of length  $N = 200$  (each Julia set is represented in one of the figure panels, from smaller to larger values of  $k$ .)

**Fig. 18** Mandelbrot slices for periodic template  $s = [011]$ . Each *panel* represents the  $c_1$  complex plane. The *panels* in the lattice was constructed for values of  $c_0$  constructed by taking partitions  $\text{Re}(c_0) = [-0.2; 0; 0.2]$  and  $\text{Im}(c_0) = [0; 0.2; 0.4; 0.6]$ . Mandelbrot slices are symmetric with respect to the real axis (not shown)



**Appendix 3: Random templates used for the figures**

$s_1 = 011100100100010011000101010011111111111$   
 $1100110010101101011011111100111010001101$   
 $001011100011010010100011000110111100000$   
 $1000101010101000000111011100011000111010$   
 $0110111011100000011111100110010010101111100$   
 $s_2 = 0100110110101001011001010001001110010011$   
 $010100100100100000011001111010001011011$   
 $1001101010110001111011010001110000100100$

$11111001111000010111010011010100011111$   
 $0101011010011100001101111100101101001000011$   
 $s_3 = 011110111111000001111000000000101001111$   
 $111001010001111111000110100111111001000$   
 $111111010001110110011000101101111000000101$   
 $1000101001110011000100000000101001100$   
 $0111011010111010111000110100011100001001011$   
 $s_4 = 0001011110111111001010101010010010111100$   
 $010000000110000011010001110000100100011$   
 $011011010010111101100000110100100001011$

0010110101010111110001001101000000011011  
 1110110010010000101101010110011110101011110

$s_5 =$  0100110110100111011011100001111100110100  
 110001000100010001001010111011010000011  
 0001001101110100111010100001111100010111  
 100001110001010010011101101111101001101  
 1010110001001101000001100100001010010001101

$s_6 =$  0100110110100111011011100001111100110100  
 110001000100010001001010111011010000011  
 0001001101110100111010100001111100010111  
 100001110001010010011101101111101001101  
 1010110001001101000001100100001010010001101

$s_7 =$  0010100011111110010010000110011111101111  
 011011110011100111101100000011001101000  
 01001011000101001101001011011110100000111  
 10000010000100000111010100111111001101  
 10001010111001111111010011011101100110000

**References**

1. Branner, B., Hubbard, J.H.: The iteration of cubic polynomials part II: patterns and parapatterns. *Acta Math.* **169**(1), 229–325 (1992)
2. Brunel, N., Latham, P.E.: Firing rate of the noisy quadratic integrate-and-fire neuron. *Neural Comput.* **15**(10), 2281–2306 (2003)
3. Carleson, L., Gamelin, T.W.: *Complex Dynamics*, vol. 69. Springer Science & Business Media, Berlin (1993)
4. Comerford, M.: Hyperbolic non-autonomous Julia sets. *Ergod. Theory Dyn. Syst.* **26**(2), 353–377 (2006)
5. Comerford, M., Woodard, T.: Preservation of external rays in non-autonomous iteration. *J. Diff. Equ. Appl.* **19**(4), 585–604 (2013)
6. Danca, M.F., Bourke, P., Romera, M.: Graphical exploration of the connectivity sets of alternated Julia sets. *Nonlinear Dyn.* **73**(1–2), 1155–1163 (2013)
7. Danca, M.F., Romera, M., Pastor, G.: Alternated Julia sets and connectivity properties. *Int. J. Bifurc. Chaos* **19**(6), 2123–2129 (2009)
8. Devaney, R.L., Look, D.M.: A criterion for Sierpinski curve Julia sets. In: *Topology Proceedings*, vol. 30, pp. 163–179 (2006)
9. Ermentrout, G.B., Kopell, N.: Parabolic bursting in an excitable system coupled with a slow oscillation. *SIAM J. Appl. Math.* **46**(2), 233–253 (1986)
10. Fatou, P.: Sur les équations fonctionnelles. *Bulletin de la Société Mathématique de France* **47**, 161–271 (1919)
11. Fornæss, J.E., Sibony, N.: Random iterations of rational functions. *Ergod. Theory Dyn. Syst.* **11**(4), 687–708 (1991)
12. Johnson, R.E., Washington, M.T., Prakash, S., Prakash, L.: Fidelity of human DNA polymerase  $\eta$ . *J. Biol. Chem.* **275**(11), 7447–7450 (2000)
13. Julia, G.: Mémoire sur l’itération des fonctions rationnelles. *J. Math. Pures. Appl.* 47–246 (1918)
14. Pray, L.: DNA replication and causes of mutation. *Nat. Educ.* **1**(1), 214 (2008)
15. Qiu, W.Y., Yin, Y.C.: Proof of the Branner–Hubbard conjecture on Cantor Julia sets. *Sci. China Ser. A Math.* **52**(1), 45–65 (2009)
16. Sester, O.: Combinatorial configurations of fibered polynomials. *Ergod. Theory Dyn. Syst.* **21**(3), 915–955 (2001)
17. Stankewitz, R., Sumi, H.: Structure of Julia sets of polynomial semigroups with bounded finite postcritical set. *Appl. Math. Comput.* **187**(1), 479–488 (2007)
18. Sumi, H.: Dynamics of sub-hyperbolic and semi-hyperbolic rational semigroups and skew products. *Ergod. Theory Dyn. Syst.* **21**(2), 563–603 (2001)
19. Sumi, H.: Semi-hyperbolic fibered rational maps and rational semigroups. *Ergod. Theory Dyn. Syst.* **26**(3), 893–922 (2006)
20. Sumi, H.: Dynamics of postcritically bounded polynomial semigroups I: connected components of the Julia sets. *Discrete Contin. Dyn. Syst. Ser. A* **29**(3), 1205–1244 (2011)
21. Sumi, H.: Dynamics of postcritically bounded polynomial semigroups II: fiberwise dynamics and the Julia sets. *J. Lond. Math. Soc.* **88**(2), 294–318 (2013)
22. Sumi, H.: Dynamics of postcritically bounded polynomial semigroups III: classification of semi-hyperbolic semigroups and random Julia sets which are Jordan curves but not quasicircles. *Ergod. Theory Dyn. Syst.* **30**(6), 1869–1902 (2010)
23. Sumi, H.: Random complex dynamics and semigroups of holomorphic maps. *Proc. Lond. Math. Soc.* **102**(1), 50–112 (2011)
24. Sumi, H.: Cooperation principle, stability and bifurcation in random complex dynamics. *Adv. Math.* **245**, 137–181 (2013)